

Yuki Kikuchi,<sup>a,b</sup> Hideyuki  
Matsunami,<sup>b,c</sup> Midori Yamane,<sup>a</sup>  
Katsumi Imada<sup>a,b,\*</sup> and  
Keiichi Namba<sup>a,b</sup>

<sup>a</sup>Graduate School of Frontier Biosciences,  
Osaka University, 1-3 Yamadaoka, Suita,  
Osaka 565-0871, Japan, <sup>b</sup>Dynamic  
NanoMachine Project, ICORP, JST,  
1-3 Yamadaoka, Suita, Osaka 565-0871, Japan, and <sup>c</sup>Trans-membrane Trafficking Unit,  
Okinawa Institute of Science and Technology,  
12-22 Suzuki, Uruma, Okinawa 904-2234,  
Japan

Correspondence e-mail:  
kimada@fbs.osaka-u.ac.jp

Received 12 September 2008  
Accepted 17 November 2008

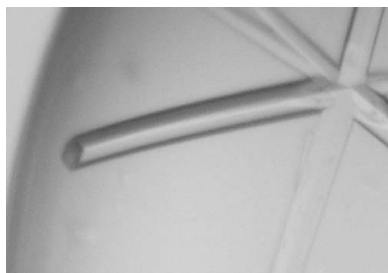
## Crystallization and preliminary X-ray analysis of a C-terminal fragment of FlgJ, a putative flagellar rod cap protein from *Salmonella*

The formation of the bacterial flagellar axial structure, including the filament, the hook and the rod, requires the attachment of a cap complex to the distal end of the growing structure. Because the rod penetrates the peptidoglycan (PG) layer, the rod cap complex is thought to have PG-hydrolyzing activity. FlgJ is a putative rod cap protein whose C-terminal region shows sequence similarity to known muramidases. In this study, FlgJ<sub>120–316</sub>, a C-terminal fragment of FlgJ which contains the muramidase region, was overproduced, purified and crystallized. Crystals were obtained by the sitting-drop vapour-diffusion technique using PEG 3350 as a crystallizing agent and belonged to the orthorhombic space group  $P2_12_12_1$ , with unit-cell parameters  $a = 38.8$ ,  $b = 43.9$ ,  $c = 108.5$  Å. Anomalous difference Patterson maps calculated from the diffraction data set of a selenomethionine-labelled crystal showed significant peaks in the Harker sections, indicating that the data were suitable for structure determination.

### 1. Introduction

The flagellum is a long filamentous organelle that is involved in bacterial motility. The flagellum is composed of basal body rings and a tubular axial structure. The basal body rings form a reversible rotary motor, which is embedded in the cell membrane and generates torque (Berg & Anderson, 1973; Silverman & Simon, 1974). The axial structure consists of three parts: the filament, the hook and the rod (DePamphilis & Adler, 1971*a,b*). The filament is a thin helical structure that typically grows to around 15 µm in length and rapidly rotates to propel the cell in viscous environments. The hook is a short curved segment of approximately 55 nm in length. The hook acts as a universal joint that smoothly transmits the motor torque to the filament regardless of its orientation. The rod is a drive shaft with an approximate length of 30 nm that connects the rotor rings and the hook. The rod penetrates the peptidoglycan (PG) layer and the outer membrane through the L–P ring complex, which works as a bushing (for review articles, see Macnab, 2003; Berg, 2003).

The flagellar axial component proteins are synthesized in the cytoplasm, transferred into the central channel of the flagellum through the flagellar type III protein-export apparatus and transported through the narrow channel to the distal end for self-assembly (Macnab, 2004; Minamino & Namba, 2004). The assembly processes of the filament and the hook are promoted by specific cap complexes composed of FlhD and FlgD, respectively (Ikeda *et al.*, 1987; Ohnishi *et al.*, 1994). These caps are both homopentameric complexes that are stably attached to the distal end of the filament or the hook and prevent leakage of their component proteins to the culture medium by capping the central channel (Ikeda *et al.*, 1985, 1987, 1996; Homma *et al.*, 1984). The transported proteins are thus efficiently incorporated into the growing structure just beneath the cap complex. The rod is also expected to require its specific cap complex for assembly. The growing rod must penetrate the PG layer; FlgH and FlgI then assemble around the rod to form the L–P ring (Kubori *et al.*, 1992). Thus, the rod cap must have PG-hydrolyzing activity in order to make a hole in the PG layer.



© 2009 International Union of Crystallography  
All rights reserved

FlgJ is a putative rod cap protein that has been found to interact with all rod-component proteins (Hirano *et al.*, 2001) and possesses PG-hydrolyzing activity (Nambu *et al.*, 1999). FlgJ is 316 amino acids long, with a molecular mass of 34.4 kDa. The C-terminal half of FlgJ shares sequence homology with other muramidases, such as autolysin, muramidase-2 and AcmA (Joris *et al.*, 1992; Buist *et al.*, 1995; Nambu *et al.*, 1999). The PG-hydrolyzing activity of FlgJ needs to be well controlled to make a hole with an appropriate size for rod formation, as the stator complexes of the flagellar motor have to be anchored in the PG layer around the basal body for torque generation (DeMot & Vanderleyden, 1994; Van Way *et al.*, 2000). To elucidate the mechanism of rod formation, we crystallized a C-terminal fragment of FlgJ, FlgJ<sub>120–316</sub>, which consists of the conserved muramidase domain (152–316) and 32 N-terminal residues unique to FlgJ (120–151). Here, we report the overproduction, purification, crystallization and preliminary X-ray crystallographic study of FlgJ<sub>120–316</sub>.

## 2. Materials and methods

### 2.1. Protein overproduction

A *NdeI/BamHI* fragment encoding FlgJ from *Salmonella enterica* serovar Typhimurium strain SJW1103 (Yamaguchi *et al.*, 1984) was amplified by PCR and inserted into the *NdeI/BamHI* site of pET3c (Novagen) to create pHMK501. *NdeI/BamHI* fragments encoding FlgJ<sub>120–316</sub> and FlgJ<sub>120–316</sub> with a C-terminal hexahistidine tag (FlgJ<sub>120–316</sub>-6×His) were then produced from pHMK501 and inserted into pET3c (pYK101) and pET22b (pYK103), respectively (Novagen). The C-terminal phenylalanine (Phe316) was substituted to

leucine to create the *BamHI* site. The vector plasmids were transformed into *Escherichia coli* strain BL21 (DE3). Cells were grown in 5 l LB medium containing 50 µg ml<sup>-1</sup> ampicillin at 310 K until the culture density reached an OD<sub>600</sub> of 0.6. IPTG was then added to a final concentration of 0.5 mM and growth continued for a further 5 h. The cells were harvested by centrifugation (6370g, 10 min, 277 K) and stored at 193 K.

### 2.2. Protein purification

Cells carrying pYK101 were thawed, suspended in 60 ml binding buffer (20 mM Na MES pH 6.0, 6 M urea) and sonicated (ASTRA-SON model XL2020 sonicator, Misonix Inc.). The cell lysate was centrifuged (145 000g, 20 min, 277 K) to remove cell debris. The soluble fraction was subjected to a HiTrap cation-exchange column (GE Healthcare) equilibrated with binding buffer. After washing the column with binding buffer, proteins were eluted using a linear gradient of 0–1 M NaCl. Fractions containing FlgJ<sub>120–316</sub> were identified by SDS-PAGE and dialyzed overnight against a buffer containing 20 mM Na HEPES pH 7.0 at 277 K to remove urea for refolding. The dialyzed sample was then centrifuged (81 800g, 10 min, 277 K) to remove aggregates. The supernatant was subjected to a HiTrap cation-exchange column equilibrated with the buffer used for dialysis. After washing the column with the same buffer, the bound proteins were eluted using a linear gradient of 0–1 M NaCl. Fractions containing FlgJ<sub>120–316</sub> were concentrated by Vivaspinn (10 000 molecular-weight cutoff, Vivascience), loaded onto a HiLoad 16/60 Superdex 75 prep-grade column (GE Healthcare) equilibrated with a buffer containing 20 mM Na HEPES pH 7.5, 150 mM NaCl and eluted at a flow rate of 1.0 ml min<sup>-1</sup>. Fractions containing FlgJ<sub>120–316</sub> were pooled, concentrated and dialyzed against a buffer containing 20 mM Na HEPES pH 7.5.

The cells carrying pYK103 were thawed, suspended in 60 ml binding buffer (50 mM Tris-HCl pH 7.5, 500 mM NaCl, 20 mM imidazole, 6 M urea) and sonicated. The cell lysate was centrifuged (145 000g, 20 min, 277 K) to remove cell debris. The soluble fraction was subjected to a HisTrap FF column (GE Healthcare) equilibrated with binding buffer. After washing the column with binding buffer, the proteins were refolded with a linear gradient of 6–0 M urea for 200 min (0.5 ml min<sup>-1</sup>) on the column. The proteins were then eluted using a linear gradient of 20–500 mM imidazole. Fractions containing FlgJ<sub>120–316</sub>-6×His were concentrated and this was followed by gel filtration as described above.

The purity of the sample was examined by SDS-PAGE and MALDI-TOF mass spectrometry (Voyager-DE PRO Workstation, Applied Biosystems). The PG-hydrolyzing activity was examined using an acrylamide gel plate containing 0.1% (w/v) micrococcus powder (Sigma). 1 µl sample solution was dropped onto the gel plate; after 6 h incubation at 310 K the plate was stained with methylene blue and washed with water. If the sample possesses PG-hydrolyzing activity, a transparent spot should appear on the blue background where the sample was dropped.

FlgJ<sub>120–316</sub> labelled with SeMet was produced in *E. coli* strain B834 (DE3) carrying pYK101 using LeMaster medium (LeMaster & Richards, 1985) containing 50 mg seleno-L-methionine instead of methionine and 5 mg thiamine per litre of culture medium. SeMet FlgJ<sub>120–316</sub> was purified using the same protocol as used for native FlgJ<sub>120–316</sub>.

### 2.3. Crystallization

Initial crystallization screening of FlgJ<sub>120–316</sub> and FlgJ<sub>120–316</sub>-6×His was performed at 277 and 293 K by the sitting-drop vapour-diffusion

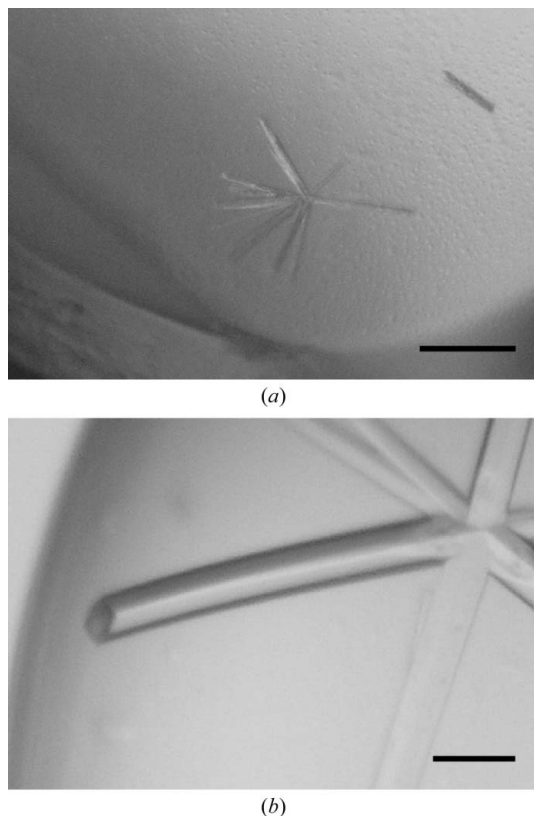


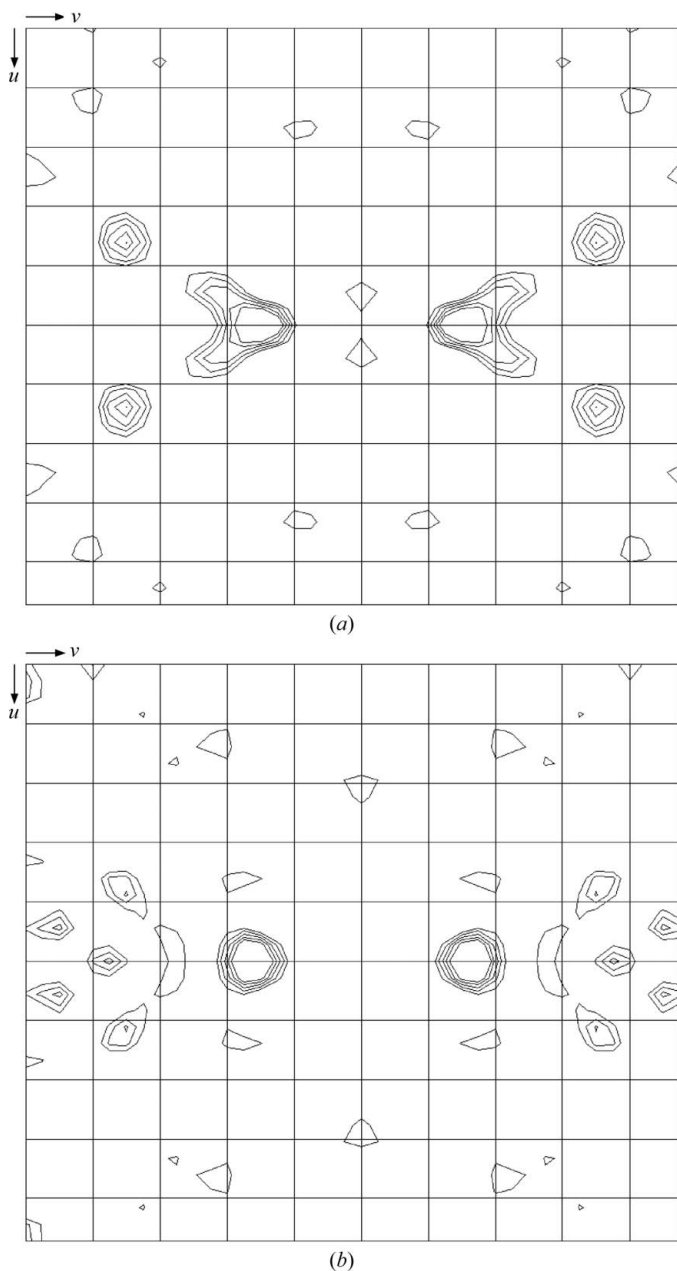
**Figure 1**  
(a) Crystals of FlgJ<sub>120–316</sub>-6×His. These thin needle-shaped crystals were obtained during initial screening. (b) Crystals of FlgJ<sub>120–316</sub>. These rod-shaped crystals were obtained after optimization. The scale bar is 0.1 mm in length.

**Table 1**

Data-collection statistics.

Values in parentheses are for the highest resolution shell.

	Native	SeMet			
		Peak	Edge	High remote	Low remote
Space group	$P2_12_12_1$	$P2_12_12_1$			
Unit-cell parameters (Å)	$a = 38.8, b = 43.9, c = 108.5$	$a = 38.8, b = 43.8, c = 108.3$			
Wavelength (Å)	1.000	0.9790	0.9794	0.972	0.986
Resolution (Å)	1.7 (1.79–1.70)	2.0 (2.11–2.00)			
Observations	143946 (20815)	113051 (14771)	113245 (14814)	103374 (14048)	102092 (12849)
Unique reflections	20999 (2970)	13011 (1804)	13031 (1810)	13048 (1838)	12964 (1762)
Completeness (%)	99.3 (99.3)	99.5 (97.9)	99.5 (97.8)	99.7 (99.2)	99.1 (95.9)
Redundancy	6.9 (7.0)	8.7 (8.2)	8.7 (8.2)	7.9 (7.6)	7.9 (7.3)
$I/\sigma(I)$	7.2 (2.6)	8.7 (5.6)	8.3 (5.3)	8.5 (5.6)	8.5 (5.2)
$R_{\text{merge}}$ (%)	6.5 (26.2)	5.5 (12.8)	5.7 (13.6)	5.4 (12.6)	5.6 (13.8)
$R_{\text{anom}}$ (%)		4.0 (6.9)	2.8 (5.7)	3.2 (6.1)	2.1 (5.5)


**Figure 2**

(a) Bijvoet and (b) dispersive Patterson maps calculated using data from the SeMet-derivative crystal. The Se peaks are shown in the  $w = 0.5$  Harker section.

technique using the following screening kits: Wizard I, II and III, Cryo I and II (Emerald BioSystems) and Crystal Screens I and II (Hampton Research). Drops were prepared by mixing 1  $\mu\text{l}$  protein solution ( $1\text{--}20\text{ mg ml}^{-1}$ ) with 1  $\mu\text{l}$  reservoir solution and were equilibrated against 200  $\mu\text{l}$  reservoir solution. After six months of incubation, clusters of thin needle-shaped crystals were grown from conditions Wizard I No. 28 and Wizard III No. 10 at 277 K (Fig. 1a) using FlgJ<sub>120–316</sub>-6 $\times$ His. At this stage, no crystals of FlgJ<sub>120–316</sub> were obtained. Therefore, we applied the microseeding technique to FlgJ<sub>120–316</sub> and FlgJ<sub>120–316</sub>-6 $\times$ His. We optimized the conditions by using additives and varying the concentration of crystallizing agents and finally obtained rod-shaped crystals of FlgJ<sub>120–316</sub> with typical dimensions of  $0.05 \times 0.05 \times 0.1\text{ mm}$  from a solution containing 0.1 M Na HEPES pH 7.5, 22–26% (v/v) PEG 3350 and 0.6–1.0 M NaCl at 277 K (Fig. 1b) within a week. SeMet-labelled crystals were obtained from the same conditions as used for the native crystals.

#### 2.4. Data collection and processing

X-ray experiments were performed on the SPring-8 beamlines BL41XU and BL38B1 (Harima, Japan). Crystals were soaked in a solution containing 90% (v/v) reservoir solution and 10% (v/v) MPD for a few seconds and immediately transferred into liquid nitrogen for freezing. Diffraction data were collected from the native crystal using an ADSC Quantum 315 CCD detector (Area Detector Systems Corporation) under a 40 K helium-gas flow on beamline BL41XU. MAD experiments on SeMet-labelled crystals were carried out on BL38B1 using a Jupiter 210 CCD detector (Rigaku/MSO) under a 100 K nitrogen-gas flow. The wavelengths for MAD measurements were selected based on XAFS measurements. The diffraction data were indexed, integrated and scaled using the programs *MOSFLM* (Leslie, 1992) and *SCALA* from the *CCP4* program suite (Collaborative Computational Project, Number 4, 1994). The statistics of data collection are summarized in Table 1.

### 3. Results and discussion

The use of highly concentrated (6 M) urea solution in the cell-disruption step was essential for crystallization of FlgJ<sub>120–316</sub>. When FlgJ<sub>120–316</sub> was purified without urea, the protein gradually degraded even in the presence of common protease inhibitors. Therefore, we applied the method developed by Saijo-Hamano *et al.* (2000) to completely suppress the activities of contaminating proteases under denaturing conditions.

The FlgJ<sub>120–316</sub> crystal diffracted to 1.7 Å resolution. The crystal belonged to the orthorhombic space group  $P2_12_12_1$ , with unit-cell

parameters  $a = 38.8$ ,  $b = 43.9$ ,  $c = 108.5$  Å. From calculation of the Matthews coefficient ( $V_M$ ; Matthews, 1968) the crystal is expected to contain one molecule per asymmetric unit, with a solvent content of 42.7%.

The SeMet FlgJ<sub>120–316</sub> crystal diffracted to 2.0 Å resolution. The unit-cell parameters of the crystals were almost the same as those of the native crystal. The statistics of the diffraction data at four different wavelengths are summarized in Table 1. The Bijvoet and dispersive difference Patterson maps of the SeMet derivative showed clear common peaks on the Harker sections (Fig. 2), suggesting the usefulness of these data for phasing by the MAD method.

We thank N. Shimizu, M. Kawamoto and K. Hasegawa at SPring-8 for technical help in the use of beamlines BL41XU and BL38B1. This work was supported in part by Grants-in-Aid for Scientific Research (20370036 to KI and 16087207 to KN) from the Ministry of Education, Science and Culture of Japan.

## References

- Berg, H. C. (2003). *Annu. Rev. Biochem.* **72**, 19–54.
- Berg, H. C. & Anderson, R. A. (1973). *Nature (London)*, **245**, 380–382.
- Buist, G., Kok, J., Leenhouts, K. J., Dabrowska, M., Venema, G. & Haandrikman, A. J. (1995). *J. Bacteriol.* **177**, 1554–1563.
- Collaborative Computational Project, Number 4 (1994). *Acta Cryst.* **D50**, 760–763.
- DeMot, R. & Vanderleyden, J. (1994). *Mol. Microbiol.* **12**, 333–334.
- DePamphilis, M. L. & Adler, J. (1971a). *J. Bacteriol.* **105**, 376–383.
- DePamphilis, M. L. & Adler, J. (1971b). *J. Bacteriol.* **105**, 384–395.
- Hirano, T., Minamino, T. & Macnab, R. M. (2001). *J. Mol. Biol.* **312**, 359–369.
- Homma, M., Fujita, H., Yamaguchi, S. & Iino, T. (1984). *J. Bacteriol.* **159**, 1056–1059.
- Ikeda, T., Asakura, S. & Kamiya, R. (1985). *J. Mol. Biol.* **184**, 735–737.
- Ikeda, T., Homma, M., Iino, T., Asakura, S. & Kamiya, R. (1987). *J. Bacteriol.* **169**, 1168–1173.
- Ikeda, T., Oosawa, K. & Hotani, H. (1996). *J. Mol. Biol.* **259**, 679–686.
- Joris, B., Englebert, S., Chu, C.-P., Kariyama, R., Daneo-Moore, L., Shockman, G. D. & Ghuyssen, J.-M. (1992). *FEMS Microbiol. Lett.* **91**, 257–264.
- Kubori, T., Shimamoto, N., Yamaguchi, S., Namba, K. & Aizawa, S.-I. (1992). *J. Mol. Biol.* **226**, 433–446.
- LeMaster, D. M. & Richards, F. M. (1985). *Biochemistry*, **24**, 7263–7268.
- Leslie, A. G. W. (1992). *Jnt CCP4/ESF-EACBM Newsl. Protein Crystallogr.* **26**.
- Macnab, R. M. (2003). *Annu. Rev. Microbiol.* **57**, 77–100.
- Macnab, R. M. (2004). *Biochim. Biophys. Acta*, **1694**, 207–217.
- Matthews, B. W. (1968). *J. Mol. Biol.* **33**, 491–497.
- Minamino, T. & Namba, K. (2004). *J. Mol. Microbiol. Biotechnol.* **7**, 5–17.
- Nambu, T., Minamino, T., Macnab, R. M. & Kutsukake, K. (1999). *J. Bacteriol.* **181**, 1555–1561.
- Ohnishi, K., Ohto, Y., Aizawa, S.-I., Macnab, R. M. & Iino, T. (1994). *J. Bacteriol.* **176**, 2272–2281.
- Saijo-Hamano, Y., Namba, K. & Oosawa, K. (2000). *J. Struct. Biol.* **132**, 142–146.
- Silverman, M. & Simon, M. (1974). *Nature (London)*, **249**, 73–74.
- Van Way, S. M., Hosking, E. R., Braun, T. F. & Manson, M. D. (2000). *J. Mol. Biol.* **297**, 7–24.
- Yamaguchi, S., Fujita, H., Sugata, K., Taira, T. & Iino, T. (1984). *J. Gen. Microbiol.* **130**, 255–265.